MAP Estimation for Spectral Image Reconstruction Using 3-band Image and Multipoint Spectral Measurements

°Kunihiko Ietomi , Yuri Murakami, Masahiro Yamaguchi, and Nagaaki Ohyama
Imaging Science & Engineering Laboratory, Tokyo Institute of Technology
4259 Nagatsuta-cho, Midori-ku, Yokohama 226-8503 Japan

Abstract

This paper presents a new spectral image reconstruction method based on MAP estimation from a 3-band image and multipoint spectral measurements. Spectral information is utilized as auxiliary information to improve the accuracy of spectral reflectance estimation from 3-band images. As a result of the preliminary experiment, it is shown that the proposed method with 81 spectral measurements reduces the color estimation error in CIELAB by about half compared to the conventional Wiener estimation method.

1. Introduction

High fidelity color reproduction is quite important in digital imaging systems for printing, telemedicine, on-line shopping, and teleconference. Spectral imaging technology is promising in order to acquire and reproduce the high-fidelity color.

For the acquisition of spectral images, multispectral imaging technique have already been developed and tested [1-4], and it has been verified that the spectral reflectance image can be estimated with high accuracy from multispectral camera. For wider use of multispectral-based color reproduction, however, it is strongly required to reduce the number of color channels to realize more compact and easy-to-use instruments.

In order to reduce the number of color channels without significant loss of accuracy, this paper focuses on utilizing multipoint spectral measurements as auxiliary information. By scanning a small spectral sensor attached to an imaging device, multipoint spectral measurements can be acquired in a practical manner. A low-resolution spectral imaging device can be also employed instead. It is expected that such auxiliary spectral data improves the estimation accuracy especially when the number of color channels is not sufficient such as conventional 3-band cameras.

The merging of imagery from two observations from different sources has been reported in the field of remote sensing; a high-resolution panchromatic image and a low-resolution spectral image are combined to generate a high-resolution spectral image. Though various methods have been proposed for that purpose [5,6], they use satellite-image-specific assumptions and cannot be applied for our purpose directly.

This paper presents an estimation method of spectral reflectance image from an image data and multipoint spectral measurements. For this purpose maximum a priori probability (MAP) estimation is applied, in which the multipoint spectral data are used as a *priori* information. Though the imaging device can be either conventional 3-band cameras or multispectral cameras, 3-band cameras are mainly considered in the following discussions, considering practical applications.

2. Mathematical Formulation of MAP

(a)Data Acquisition Model

The proposed method is based on the image acquisition system consisting of two observations; a high-resolution 3-channel image and multipoint spectrum measurements. Let us formulate the data acquisition model of the system in this section. In the

formulation, it is assumed that a high-resolution 3-channel image with no spatial degradation and low-resolution multipoint spectral data with no spectral degradation are obtained from the same original image of spectral reflectance, **f**.

The 3-channnel imaging system can be modeled as a linear system as

$$\mathbf{g}_i = \mathbf{H}_S \mathbf{f}_i + \mathbf{n}_i \tag{1}$$

where $\mathbf{g}_i$ is a 3-dimensional column vector representing the 3-channel image signal at the spatial location designated by the index *i*, and $\mathbf{f}_i$ is a *L*-dimensional column vector representing the spectral reflectance corresponding to $\mathbf{g}_i$, respectively. $\mathbf{H}_S$ is a $3 \times L$ system matrix determined by the spectral sensitivity of the camera and the illumination spectrum, where subscript *S* means that the matrix represents *Spectral* characteristics, and $\mathbf{n}_i$ is a 3-dimensional column vector representing noise, which is assumed to be a zero-mean Gaussian random white noise. Note that the spectral characteristics of the imaging system are assumed to be spatially invariant in eq.(1). By raster scanning the two-dimensional image, we can write the system model for all *N* pixels as

$$\mathbf{g} = \mathbf{A}_S \mathbf{f} + \mathbf{n}_G \tag{2}$$

where

$$\mathbf{g} = \begin{pmatrix} \mathbf{g}_1 \\ \vdots \\ \mathbf{g}_N \end{pmatrix}, \mathbf{f} = \begin{pmatrix} \mathbf{f}_1 \\ \vdots \\ \mathbf{f}_N \end{pmatrix}, \mathbf{n}_G = \begin{pmatrix} \mathbf{n}_1 \\ \vdots \\ \mathbf{n}_N \end{pmatrix} \tag{3}$$

and

$$\mathbf{A}_S = (\mathbf{I}_N \otimes \mathbf{H}_S) = \begin{pmatrix} \mathbf{H}_S & & \mathbf{0} \\ & \ddots & \\ \mathbf{0} & & \mathbf{H}_S \end{pmatrix} \tag{4}$$

where $\mathbf{I}_N$ is an $N \times N$ identity matrix and $\otimes$ means Kronecker product. The dimension of matrix $\mathbf{A}_S$ is $3N \times LN$.

Next, a multipoint spectral measurement system is modeled using the as

$$\mathbf{r} = \mathbf{A}_P \mathbf{f} + \mathbf{n}_R \tag{5}$$

$$\mathbf{r} = \begin{pmatrix} \mathbf{r}_1 \\ \vdots \\ \mathbf{r}_K \end{pmatrix} \tag{6}$$

$$\mathbf{A}_P = \mathbf{H}_P \otimes \mathbf{I}_L \tag{7}$$

where $\mathbf{r}_k$ is an *L*-dimensional column vector representing the spectral reflectance function measured at *k*-th measurement spot, *K* is the number of the measurement spots and $\mathbf{H}_P$ is a $K \times N$ matrix whose *k*-th row vector represents the spatial sensitivity of *k*-th measurement spot; the subscript *P* means this matrix represents *Position* of the measurement spots. In this case, the spatial sensitivity is assumed to be independent to the wavelength. The *LK*-dimensional column vector $\mathbf{n}_R$ represents a noise and it is assumed to be a Gaussian random white noise.

(b)Maximum a posteriori probability estimation

In order to estimate spectral reflectance image **f** from the two observations **g** and **r**, MAP estimation is applied. MAP estimate is obtained by maximizing the conditional probability relative to the two observations

$$P(\mathbf{f} \mid \mathbf{g}, \mathbf{r}) \tag{8}$$

Using Bayes' rule, the conditional probability density function can be expressed as

$$P(\mathbf{f} \mid \mathbf{g}, \mathbf{r}) \propto P(\mathbf{g} \mid \mathbf{f}) P(\mathbf{r} \mid \mathbf{f}) P(\mathbf{f}) \tag{9}$$

The conditional density function $P(\mathbf{g} \mid \mathbf{f})$ can be derived from the observation model. Given **f**, the high-resolution observation vector **g** has a mean of $\mathbf{A}_S \mathbf{f}$ and the variation is due only to the noise $\mathbf{n}_G$. Thus, we obtain

$$P(\mathbf{g} \mid \mathbf{f}) = C_G \exp\left[-\frac{1}{2} (\mathbf{g} - \mathbf{A}_S \mathbf{f})^T \Sigma_{NG}^{-1} (\mathbf{g} - \mathbf{A}_S \mathbf{f}) \right] \tag{10}$$

where C_G is a normalization constant and Σ_{NG} is the covariance matrix of noise $\mathbf{n}_G$. Similarly, the conditional density function of the spectral measurements becomes

$$P(\mathbf{r} \mid \mathbf{f}) = C_R \exp\left[-\frac{1}{2} (\mathbf{r} - \mathbf{A}_P \mathbf{f})^T \Sigma_{NR}^{-1} (\mathbf{r} - \mathbf{A}_P \mathbf{f}) \right] \tag{11}$$

where C_R is a normalization constant and Σ_{NR} is the covariance matrix of noise $\mathbf{n}_R$. A prior probability $P(\mathbf{f})$ is unknown but we assumed it is normally distributed;

Copyright 2007

$$P(\mathbf{f}) = C_F \exp\left[-\frac{1}{2}\left(\mathbf{f}-\bar{\mathbf{f}}\right)^T \Sigma^{-1}\left(\mathbf{f}-\bar{\mathbf{f}}\right)\right] \quad (12)$$

where C_F is a normalization constant, $\bar{\mathbf{f}}$ and Σ are the mean and the covariance matrix of **f**.

For the maximization of eq (9), following three assumptions are introduced to derive the estimation in a useful form. The first one is that the correlation between the elements of **f** is separable into the product of spatial and spectral correlation functions; the covariance matrix of **f** can be expressed as the Kronecker product of spatial covariance matrix Σ_P and spectral covariance matrix Σ_S:

$$\Sigma = \Sigma_P \otimes \Sigma_S \quad (13)$$

The second assumption is that the measurement systems are noise free; Σ_{NR} and Σ_{NG} are zero matrices. The third assumption is that the mean of a priori probability of **f** is zero.

Basing on these assumptions, we derived the estimation $\hat{\mathbf{f}}$ which maximizes the eq. (9) as

$$\hat{\mathbf{f}} = (\mathbf{I}_N \otimes \mathbf{M}_S)\mathbf{g} + [\mathbf{M}_P \otimes (\mathbf{I}_L - \mathbf{M}_S\mathbf{H}_S)] \quad (14)$$

where

$$\mathbf{M}_P \equiv \Sigma_P \mathbf{H}_P{}^T \left(\mathbf{H}_P \Sigma_P \mathbf{H}_P{}^T\right)^{-1} \quad (15)$$

$$\mathbf{M}_S \equiv \Sigma_S \mathbf{H}_S{}^T \left(\mathbf{H}_S \Sigma_S \mathbf{H}_S{}^T\right)^{-1} \quad (16)$$

Extracting the estimated reflectance of the *i*-th pixel from eq. (18), we have

$$\hat{\mathbf{f}}_i = \mathbf{M}_S \mathbf{g}_i + \sum_{k=1}^{K} [\mathbf{M}_P]_{ik} (\mathbf{I}_L - \mathbf{M}_S\mathbf{H}_S)\mathbf{r}_k \quad (17)$$

The first term of eq. (17) corresponds to the normal pixel-by-pixel Wiener estimation from 3-band image signal $\mathbf{g}_i$. On the other hand, the term $(\mathbf{I}_L - \mathbf{M}_S\mathbf{H}_S)\mathbf{r}_k$ corresponds to the Wiener estimation error for the measured spectral reflectance $\mathbf{r}_k$. It is weighted by the elements of the matrix $\mathbf{M}_P$ and added to the first term. It can be said that the estimation error in the first term can be compensated by the second term, which is the spatial Wiener restoration from the multipoint spectral data.

(c)A priori probability

The estimation of eq. (14) requires a priori probability $P(\mathbf{f})$, or more specifically, spatial and spectral covariance matrices, Σ_P and Σ_S in eqs. (15) and (16). In the experiment described in the section 3, the covariance matrices were given based on the two observations as follows; the spectral covariance Σ_S is directly calculated from all measured spectral reflectance functions:

$$\Sigma_S = \frac{1}{K}\sum_{k=1}^{K} \mathbf{r}_k \mathbf{r}_k{}^T \quad (18)$$

The (*i*, *j*) element of the spatial covariance Σ_P is estimated by

$$[\Sigma_P]_{ij} = \mathbf{g}_i{}^T \mathbf{g}_j \times 0.9995^{d(i,j)} \quad (19)$$

where $d(i,j)$ is the Euclid distance between *i*-th and *j*-th pixels. This definition is based on the following idea. The (*i*, *j*) element of the spatial covariance can be seen to represent the correlation between *i*-th and *j*-th pixels. It can be measured by the inner product between image-signal vectors of *i*-th and *j*-th pixels. Besides, it can be thought that nearer pixels have higher correlation. Such effect is accounted by multiplying $0.9995^{d(i,j)}$ to the inner product.

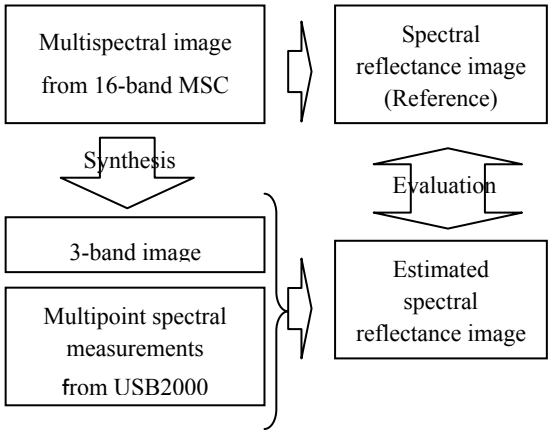

Fig. 1. Experimental procedure.

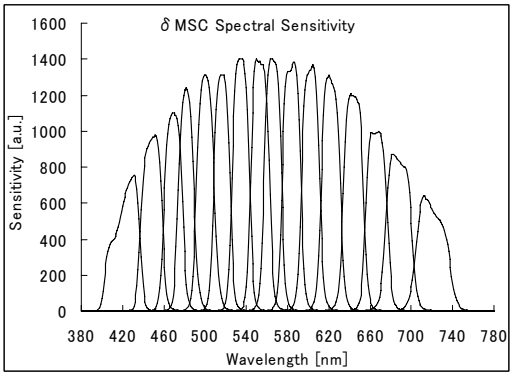

Fig. 2. Spectral sensitivity of 16-band multispectral camera used in the experiments.

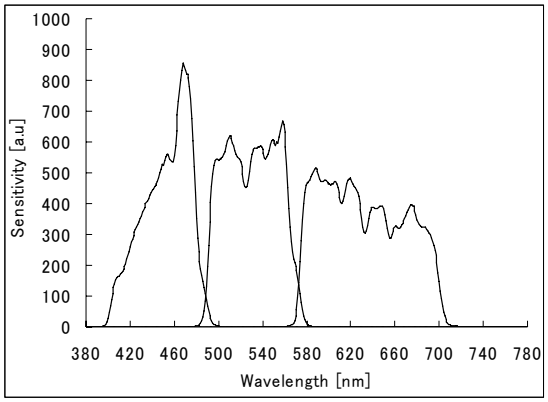

Fig. 3. Spectral sensitivity of the synthesized 3-band camera.

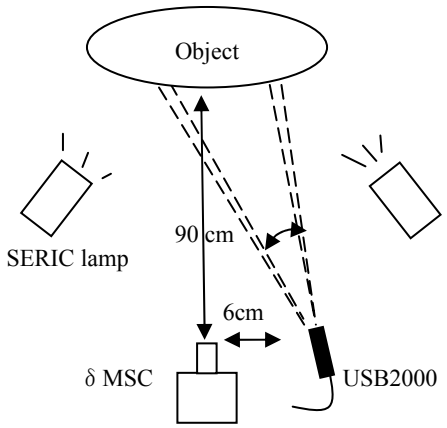

Fig. 4. Experimental arrangement.

(a) (b)

Fig. 5. Two subjects used in the experiments: 'Toy' (left) and 'Flower' (right).

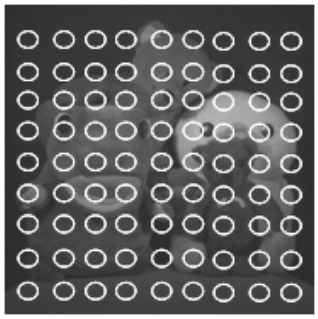

Fig.6 The position of the measurement spots.

3. Experiments

This section presents the experimental results to demonstrate the effectiveness of the proposed MAP estimation.

Experimental Procedure

The experimental procedure is illustrated in fig.1. Images were captured by the 16-band multispectral camera (δMSC, developed by Telecommunication Advancement Organization, Akasaka Natural Vision Research Center) [3]. The camera consisted of a 2048×2048 pixel monochrome CCD and a rotational wheel with 16 interference filters whose spectral sensitivities span the visible spectrum region as shown in fig. 2. The spectral reflectance was estimated from the 16-band images by Wiener estimation and they were used as a reference to evaluate the estimation results from 3-band images.

3-band images were virtually generated from the 16-band images by combining 5 to 6 adjacent bands. The synthesized 3-band spectral sensitivity is shown in fig. 3.

The experimental arrangement is shown in fig. 4. We prepared two set of objects, 'Toys' and 'Scarf' which are shown in fig. 5. They are illuminated with two daylight lamps (SOLAX 100W, SERIC) with UV filter. The Spectral radiance of the lamp was measured in advance.

USB2000 fiber-optic spectral sensor from Ocean Optics was employed to measure the multipoint spectral information. A collimator lens was attached to the end of the optical fiber and the fiber was fixed to a two-axis swivel base for scanning the measurement spot in a scene.

Spectral measurements were obtained from 81 points at about even intervals for each object. Figure 6 illustrates the rough positions and size of the measurement spots.

Spectral Estimation Methods

The following methods are compared for spectral reflectance estimation:

Wiener(Markov): the Wiener estimation of spectral reflectance from the synthesized 3-band image,

Copyright 2007

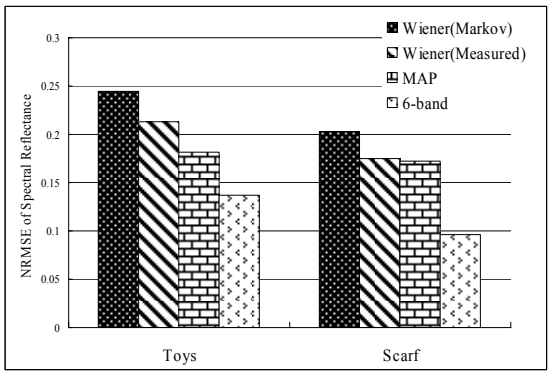

Fig.7. NRMSE of Spectral Reflectance 380-700nm

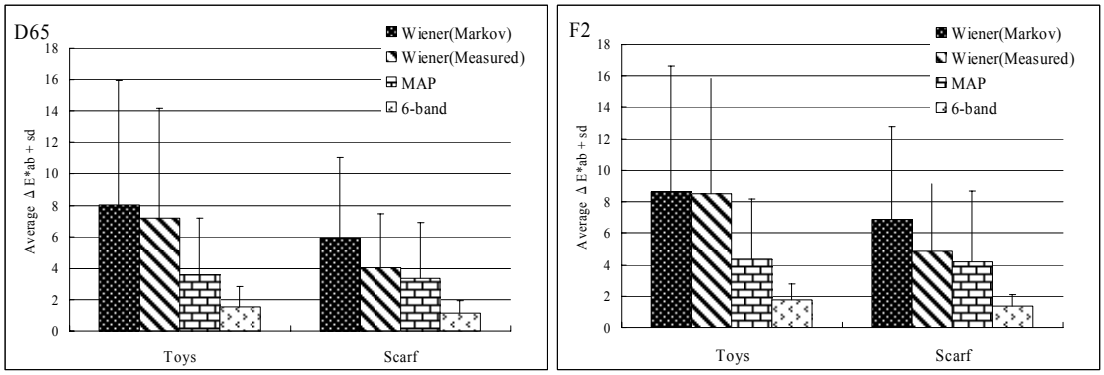

Fig.8. Average and the standard deviation (sd) of ΔE*ab under the illumination D65 (left) and F2 (right).

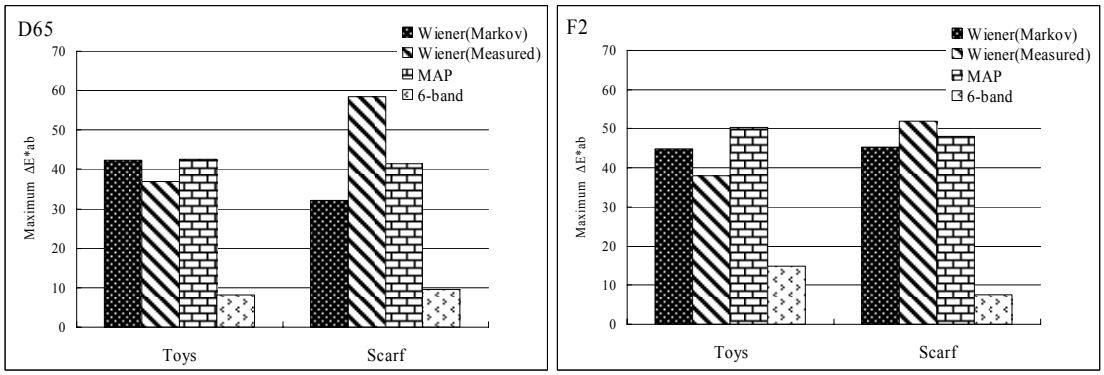

Fig.9. Maximum ΔE*ab under the illumination D65 (left) and F2 (right).

Fig.10. Visualized ΔE^*_{ab} image, where 8-bit pixel value corresponds to $\Delta E^*_{ab} \times 15$. The upper row is the results of 'Toy' and the lower row is the results of 'Scarf'.

where the correlation matrix is formulated based on Markov process of $\rho = 0.995$.

Wiener(Measured): the Wiener estimation of spectral reflectance from the synthesized 3-band image, where the correlation matrix is captured from all measured spectral reflectance functions as eq. (18).

MAP: the proposed MAP estimation from the synthesized 3-band image and the spectral measurements. This is the proposed method represented by eq. (14)/(17).

6-band: the Wiener estimation from 6-band image that is virtually generated from the 16-band image. This corresponds the 6-band version of the case Wiener(Markov). The correlation matrix is formulated based on Markov process of $\rho = 0.995$.

4. Results

Fig.7 presents the NRMSE of estimated spectral reflectance (380-700nm) for the four estimation methods. For both subjects, Wiener(Measured) reduced NRMSE compared to Wiener(Markov) due to the measured spectral reflectance. In 'Toys', further reduction was achieved by MAP; NRMSE was reduced to 74% comparison with Wiener(Markov).

Fig.8 shows the results of color reproduction accuracy. To generate the color images, the CIE 1931 XYZ color matching functions and the illumination spectrum of CIE standard illuminant D65 or F2 were employed.

The colorimetric error was evaluated by the CIELAB color difference between the color image obtained from the 16-band data and the estimated image, referred to as ΔE^*_{ab}. The average and the standard deviation (sd) of ΔE^*_{ab} under D65 and F2 illuminations are shown in fig.7. While Wiener(Measured) did not improve the accuracy in 'Toys', MAP reduces the average and sd ΔE^*_{ab} for both subjects; average ΔE^*_{ab} was reduced by almost half compared to Wiener(Markov).

Fig.9 shows the maximum ΔE^*_{ab} under D65 and F2. Maximum ΔE^*_{ab} was not reduced even when the spectral information was utilized by Wiener(Measure) or MAP.

Fig.10 demonstrates ΔE^*_{ab} images for the four methods under F2 illumination, where 8-bit pixel value corresponds to $\Delta E^*_{ab} \times 15$. We can see that MAP improves the color accuracy especially for the two subjects in the front row of 'Toy' and lower-right corner of 'Scarf'. However, there are some small areas where the error is higher than that of Wiener(Markov). It can be considered that the error was mainly caused by the parallax between the camera and the spectral measurement. Also the error becomes relatively larger when the area size of uniform color is too small. Since the human vision is less sensitive to the chromatic error in a small region, further evaluation is needed with taking account of the human visual system characteristics.

5. Conclusion

This paper presents an estimation method of spectral reflectance image from a high-resolution 3-band image and low-resolution multipoint spectral measurements based on MAP estimation. The derived solution is composed of two terms; the Wiener estimation for the spectral reflectance from a 3-band image signal and the term to compensate the Wiener estimation error based on the measured spectral information. Experimental results show that the MAP estimation reduces the average ΔE^*_{ab} up to about half with 81 spot measurements compared to the conventional Wiener estimation. The reduction of the computational cost and the optimization of the use of a *priori* information are the issue for the future investigation.

References

1. P. D. Berns and R. S. Berns, "Analysis of multispectral image capture," Proc. 4th CIC, 19-22(1996).
2. M. Yamaguchi, R. Iwama, Y. Ohya, T. Obi, N. Ohyama, Y. Komiya and T. Wada, "Natural color reproduction in the television system for telemedicine," Proc. SPIE, 3031, 482-289 (1997).
3. M. Yamaguchi, H. Haneishi, H. Fukuda, J.

Copyright 2007

4. Koshimoto, H. Kanazawa, M. Tsuchida, R. Iwama, and N. Ohyama, “High-fidelity video and still-image communication based on spectral information: Natural Vision system and its applications,” Proc. SPIE 6062, (2006)
5. K. Ohsawa, T. Ajito, H. Fukuda, Y. Komiya, H. Haneishi, M. Yamaguchi and N. Ohyama, “Six-band HDTV camera system for spectrum-based color reproduction,” J. Imag. Sci. and Tech., 48(2), 85-92 (2004).
6. D. P. Filiberti, S. E. Marsh and R. A. Schowengerdt, “Syntehsis of imagery with high spatial and spectral resolution from multiple image sources,” Optical Engineering, 33(8), 2520-2528 (1994).
7. R. C. Hardie, M. T. Eismann and G. L. Wilson, “MAP estimation for hyperspectral image resolution enhancement using an auxiliary sensor,” IEEE Trans. Image Processing, 13(9), 1174-1184 (2004).
8. A. K. Jain, “Fundamentals of digital image processing,” Prentice-Hall, Inc. 1989, P.3